A Product Formed from Glycylglycine in the Presence of Vanadate and Hydrogen Peroxide: The (Glycylde-*N*-hydroglycinato-κ^3N^2,N^N,O^1)oxoperoxovanadate(V) Anion

Frederick W. B. Einstein, Raymond J. Batchelor, Sarah J. Angus-Dunne,[†] and Alan S. Tracey*

Department of Chemistry, Simon Fraser University, Burnaby, BC V5A 1S6, Canada

Received August 2, 1995[⊗]

A crystalline glycylglycine complex of monoperoxovanadate has been obtained and its X-ray structure determined. The coordination is pentagonal bipyramidal with the peroxo group and a tridentate glycylglycine occupying the equatorial positions. The axial positions of the anion are occupied by the oxo ligand and by one oxygen of the peroxo group of the adjacent anion. The latter interaction establishes the seventh bond and produces a dimeric structure in the crystalline material. NMR studies of its dissolution in water combined with previously reported results from equilibrium measurements show that the dimer dissociates in water to the monomeric precursor. It is proposed that this monomer corresponds to the complex responsible for the inhibition of the vanadium-catalyzed decomposition of hydrogen peroxide by glycylglycine. Crystal structure of $[NEt_4][VO(O_2)(GlyGly)]\cdot 1.58H_2O$: monoclinic, space group $P2_1$; $Z = 4$; $a = 10.618(2)$ Å; $b = 14.803(2)$ Å; $c = 11.809(2)$ Å; $\beta = 101.37(2)°$; $V = 1819.7$ Å^3; $T = 198$ K; $R_F = 0.029$ for 2664 data ($I_o \geq 2.5\sigma(I_o)$) and 431 variables.

Introduction

The chemistry of peroxovanadates has been attracting interest for many years.[1] Early work focused on two areas. X-ray structure studies were concerned with defining the nuances of the coordination of hydrogen peroxide.[2−4] Other work concentrated on attempting to understand the mechanism of vanadate-catalyzed oxidation of halides[5,6] and the associated disproportionation of hydrogen peroxide into oxygen and water.[7,8]

Interest in the biochemical properties of peroxovanadates was stimulated when vanadium-dependent haloperoxidases were discovered in various marine algae[9] and in a lichen.[10] Recent review articles have discussed, in some detail, the chemistry and biochemistry of peroxovanadates.[1,11] Reports of the insulin-mimetic properties of peroxovanadium complexes stimulated even greater interest in these materials.[12−14]

^{51}V nuclear magnetic resonance spectroscopy has provided a powerful tool for the study of the solution properties of peroxovanadates and of their interactions with potential ligands.[15−17] In view of the haloperoxidase and insulin-mimetic properties associated with peroxovanadates, recent solution studies of these materials have been directed toward the reactions of peroxovanadates with ligands that form products of potential biochemical significance.[18,19]

Our interest in the peroxovanadates has concentrated principally on their reactions with biogenic materials. ^{51}V NMR studies have established the stoichiometry of the reactions of mono- and diperoxovanadium complexes with various amino acids[20] and dipeptides.[21,22] These studies have provided product formation constants and revealed the pH-dependence of product formation. One interesting result from these studies was the finding that simple dipeptides such as glycylglycine essentially completely eliminated the vanadium-catalyzed decomposition of hydrogen peroxide by forming a stable complex with monoperoxovanadate.[21,22] A product thought to correspond to this material has now been obtained in crystalline form. An X-ray structure analysis has been carried out and the structural parameters obtained. Dissolution studies have been carried out in an effort to confirm that the crystalline material corresponds to the solution product.

Experimental Section

Materials. Vanadium pentoxide (99.99%) was obtained from Aldrich Chemical Company, hydrogen peroxide (3%) from Fischer

[†] Present address: Institut für Anorganische, Organische und Physikalische Chemie, Universität Bern, Freiestrasse 3, CH-3012 Bern, Switzerland.

[⊗] Abstract published in *Advance ACS Abstracts,* February 15, 1996.

(1) Butler, A.; Clague, M. J.; Meister, G. E. *Chem. Rev.* **1994**, *94*, 625−638.
(2) Svensson, I.-B.; Stomberg, R. *Acta Chem. Scand.* **1971**, *25*, 898−910.
(3) Drew, R. E.; Einstein, F. W. B. *Inorg. Chem.* **1973**, *12*, 829−835.
(4) Drew, R. E.; Einstein, F. W. B. *Inorg. Chem.* **1972**, *11*, 1079−1083.
(5) Secco, F. *Inorg. Chem.* **1980**, *19*, 2722−2725.
(6) Clague, M. J.; Butler, A. *J. Am. Chem. Soc.* **1995**, *117*, 3475−3484.
(7) Dean, G. A. *Can. J. Chem.* **1961**, *39*, 1174−1183.
(8) Bonchio, M.; Conte, V.; Di Furia, F.; Modena, G.; Moro, S.; Edwards, J. O. *Inorg. Chem.* **1994**, *33*, 1631−1637.
(9) de Boer, E.; van Kooyk, Y.; Tromp, M. G. M.; Plat, H.; Wever, R. *Biochim. Biophys. Acta* **1986**, *869*, 48−53.
(10) Plat, H.; Krenn, B. E.; Wever, R. *Biochem. J.* **1987**, *248*, 277−279.
(11) Vilter, H. Vanadium-Dependent Haloperoxidases. In *Vanadium and its Role for Life*; Sigel, H., Sigel, A., Eds.; Metal Ions in Biological Systems; Marcel Dekker, Inc.: New York, 1995; pp 325−362.
(12) Kadota, S.; Fantus, I. G.; Deragon, G.; Guyda, H. J.; Hersh, B.; Posner, B. I. *Biochem. Biophys. Res. Commun.* **1987**, *147*, 259−266.
(13) Heffetz, D.; Bushkin, I.; Dror, R.; Zick, Y. *J. Biol. Chem.* **1990**, *265*, 2896−2902.
(14) Orvig, C., Thompson, K. H., Battell, M. and McNeill, J. H. Vanadium Compounds as Insulin Mimetics. In *Vanadium and its Role for Life*; Eds.; Sigel, H., Sigel, A., Eds.; Metal Ions in Biological Systems; Marcel Dekker, Inc.: New York, 1995, pp 575−594.
(15) Harrison, A. T.; Howarth, O. W. *J. Chem. Soc. , Dalton Trans.* **1985**, 1173−1177.
(16) Campbell, N. J.; Dengel, A. C.; Griffith, W. P. *Polyhedron* **1989**, *8*, 1379−1386.
(17) Jaswal, J. S.; Tracey, A. S. *Inorg. Chem.* **1991**, *30*, 3718−3722.
(18) Schwendt, P.; Tyrselova, J.; Pavelcik, F. *Inorg. Chem.* **1995**, *34*, 1964−1966.
(19) Bhattacharjee, M.; Chaudhuri, M. K.; Islam, N. S.; Paul, P. C. *Inorg. Chim. Acta* **1990**, *169*, 97−100.
(20) Tracey, A. S.; Jaswal, J. S. *Inorg. Chem.* **1993**, *32*, 4235−4243.
(21) Jaswal, J. S.; Tracey, A. S. *J. Am. Chem. Soc.* **1993**, *115*, 5600−5607.
(22) Tracey, A. S.; Jaswal, J. S. *J. Am. Chem. Soc.* **1992**, *114*, 3835−3840.

0020-1669/96/1335-1680$12.00/0

Scientific Co. and tetraethylammonium hydroxide from Sigma Chemical Company. The water used for the synthesis and for NMR sample preparation was deionized and then distilled.

Synthesis of $[NEt_4][VO(O_2)(GlyGly)]\cdot 1.58H_2O$. To 0.46 g of V_2O_5 (2.5 mmol) in a 10 mL beaker was added 3.5 mL of 20% aqueous Et_4NOH and approximately 1 mL of H_2O. The resultant slurry was warmed (60 °C), with stirring, until all the V_2O_5 was dissolved (about 2 h). The resultant solution was transferred to a 25 mL beaker and diluted to 10 mL (pH 10). To this solution was added 0.66 g glyclyglycine (5.0 mmol) dissolved in 5.75 mL of 0.87 M H_2O_2 (5.0 mmol). The pH of the resultant dark orange solution solution was 6.8. The solution was stirred and heated gently for 30 min, the temperature never exceeding 65 °C. The red solution was then kept at 3 °C and left uncovered to allow for slow evaporation of the water. Orange crystals, that are stable in air at 3 °C, were obtained after about 8 weeks. If dried under vacuum for 4 h, the crystals are stable at room temperature for at least a week. Yield; approximately 30% with no attempt for optimization of the reaction or cystallization procedures.

NMR Spectroscopy. ^{51}V NMR spectra were obtained at 105.2 MHz using a Bruker AMX-400 NMR spectrometer. Chemical shifts are quoted relative to an external sample of neat $VOCl_3$. Material from the isolated crystalline mass was powdered and placed in an NMR tube. Water at 276 K was added and the mixture shaken. The powder dissolved within a few seconds, and a ^{51}V NMR spectrum, also measured at 276 K, was immediately obtained. A single signal at −649 ppm was found. This signal was monitored over a time span of several hours but no changes in the spectrum were observed.

X-ray Structure Determination. A pale orange colored plate-shaped crystal was removed from the mother liquor and was cleaved to yield a single crystal fragment of suitable size. With a trace of Apiezon grease as adhesive, the fragment was gently wedged inside a glass capillary tube, which was then sealed. Data were recorded at 198 K with an Enraf Nonius CAD4F diffractometer equipped with an in-house modified low-temperature attachment and using graphite monochromatized Mo Kα radiation. Two standard reflections were measured every hour of exposure time and fluctuated in intensity by ±3% during the course of the measurements. The data were corrected for absorption by the Gaussian integration method. Data reduction included corrections for intensity scale variation and for Lorentz and polarization effects.

A number of weak reflections, which violated the systematic condition for a *c*-glide plane in the space group $P2_1/c$, were observed. As a consequence, after the data collection was completed, the sample was warmed to room temperature and a selection of expected *h*0*l* (*l*-odd) reflections were measured for but were not found. After recooling to 198 K, they were again observed.

After the initial structural refinement was completed and in order to substantiate the noncentrosymmetric space group symmetry, further data were collected. This required the preparation of a new crystalline sample as the original crystal had degraded. A crystal of high quality (0.22 × 0.22 × 0.37 mm) was selected and cooled to approximately the same temperature as for the first measurements. The second crystal had unit cell dimensions of $a = 10.619(2)$ Å, $b = 14.806(4)$ Å, $c = 11.775(2)$ Å, and $\beta = 101.14(2)°$ at 202 K. The apparent slight contractions of the *c*-dimension and β-angle compared to those of the original crystal (see Table 1) are possibly consequences of a slightly different water content. Forty-five sets of indices, for which the Friedel inequivalent structure factors were predicted to show the most significant differences (ranging in magnitude from $25\sigma(F_o)$ down to $5\sigma(F_o)$) based on the refined structure in $P2_1$, were selected. Both symmetry equivalent and Friedel related reflections were measured.

When the diffraction pattern of the second crystal was obtained, it showed the same violations of the *c*-glide systematic condition as that of the original crystal. In every case, the sign of the difference between observed Friedel-related structure factors was consistent with that predicted by the structural model. This potentially pyroelectric behavior suggests that this compound may warrant further study as a possible ferroelectric.

Despite the weakly observed reflections that violated the systematic condition for a *c*-glide plane, the structure was initially solved in the space group $P2_1/c$. The best structure factor agreement obtained in $P2_1/c$ was $R = 0.088$ with an ordered model and anisotropic thermal parameters for all non-hydrogen atoms. In this model one of the two independent water molecules showed fractional occupancy of about 0.6.

Table 1. Crystallographic Data for the Structure Determination of $[NEt_4][VO(O_2)(GlyGly)]\cdot 1.58H_2O$ at 198 K

formula	$VO_{7.58}N_3C_{12}H_{29.16}$	cryst syst	monoclinic
fw	387.76	space group	$P2_1$
a (Å)[a]	10.618(2)	ρ_c (g cm^{-3})	1.415
b (Å)	14.803(2)	λ(Mo Kα_1) (Å)	0.70930
c (Å)	11.809(2)	μ(Mo Kα) (cm^{-1})	5.6
β (deg)	101.37(2)	min−max 2θ (deg)	4−50
V (Å^3)	1819.7	transm[b]	0.810−0.914
Z	4	cryst dimens (mm)	0.16 × 0.39 × 0.41
temp (K)	198	GoF[c]	2.07
R_F[d]	0.029	R_{wF}[e]	0.035

[a] Cell dimensions were determined from 25 reflections ($36° \le 2\theta \le 46°$). [b] The data were corrected for the effects of absorption by the Gaussian integration method. [c] $\text{GoF} = [\sum(w(F_o - F_c)^2)/\text{degrees of freedom}]^{1/2}$. [d] $R_F = \sum||F_o| - |F_c||/\sum|F_o|$, for 2664 data ($I_o \ge 2.5\sigma(I_o)$). [e] $R_{wF} = [\sum(w(|F_o| - |F_c|)^2)/\sum(wF_o^2)]^{1/2}$ for 2664 data ($I_o \ge 2.5\sigma(I_o)$); $w = [\sigma(F_o)^2 + 0.0001F_o^2]^{-1}$.

With the use of distance and thermal motion restraints, a model was developed in the space group $P2_1$ that involved two independent anions, two independent cations and four independent water sites. Only one of the water sites (O(8)) showed reduced refined fractional occupancy (0.16(1)) consistent with the reduced symmetry.

Hydrogen atoms of the ions, while located in an electron density difference map, were nonetheless included in calculated positions with isotropic temperature factors initially dependent on the equivalent isotropic temperature factor of their associated C- or N-atoms. All but one of the hydrogen atoms of the full occupancy water molecules were located at peaks in an electron density difference map. The remaining full hydrogen atom (on O(28)) as well as fractional hydrogen atoms (on O(8)) were placed at interpolated positions consistent with the only plausibly hydrogen-bonded O--O interactions involving these water molecules. All hydrogen atoms were made to ride on their respective C-, N-, or O-atoms during refinement. A single parameter was refined for the isotropic thermal motion of the water hydrogen atoms and another for all other hydrogen atoms in the structure. Anisotropic thermal parameters for all non-hydrogen atoms were refined. All restraints, except for one restraining the sum of all *y*-coordinates—to prevent a singularity because of the unfixed origin along the polar axis—were released in the final cycles of full-matrix least-squares refinement.

A weighting scheme based on counting statistics was applied such that $\langle w(|F_o| - |F_c|)^2\rangle$ was nearly constant as a function of both $|F_o|$ and $(\sin\theta)/\lambda$. Final full-matrix least-squares refinement of 431 parameters for 2664 data ($I_o \ge 2.5\sigma(I_o)$) and one restraint converged at $R = 0.029$. The final maximum |shift/error| was 0.01. Crystallographic details are summarized in Table 1. Final fractional atomic coordinates for the non-hydrogen atoms are listed in Table 2. The computer programs used were from the *NRCVAX* Crystal Structure System[23] and from *CRYSTALS*[24] which was used for the structure refinement. Complex scattering factors for neutral atoms[25] were used in the calculation of structure factors. Computations were carried out on MicroVAX-II and 80486 computers.

Analysis of the anisotropic thermal parameters using a rigid-body[26] model for each ion yielded $R = 0.138$, 0.140, 0.094, and 0.101 for the agreement between observed and calculated U_{ij} for the two anions and cations, respectively, and an rms discrepancy of 0.003 Å^2 in each case. The resultant corrected bond lengths are included in Table 3.

(23) Gabe, E. J.; LePage, Y.; Charland, J.-P.; Lee, F. L.; White, P. S. *J. Appl. Cryst.* **1989**, *22*, 384.
(24) Watkin, D. J.; Carruthers, J. R.; Betteridge, P. W. *CRYSTALS*; Chemical Crystallography Laboratory, University of Oxford: Oxford, England, 1984.
(25) *International Tables for X-ray Crystallography*; Kynoch Press: Birmingham, 1975; Vol. IV, p 99.
(26) Shomaker, V.; Trueblood, K. N. *Acta Crystallogr.* **1968**, *B24*, 63−76.

Table 2. Fractional Atomic Coordinates and Equivalent Isotropic Temperature Factors (Å^2) for the Non-Hydrogen Atoms of $[NEt_4][VO(O_2)(GlyGly)]\cdot 1.58H_2O$ at 198 K

atom	*x*	*y*	*z*	U_{eq}[a] (Å^2)	atom	*x*	*y*	*z*	U_{eq}[a] (Å^2)
V(1)	0.59247(8)	0.10568(10)	0.27332(6)	0.0211	C(1)	0.7072(5)	0.1067(4)	0.5174(4)	0.0279
V(2)	0.59676(8)	0.39821(10)	0.76569(6)	0.0210	C(2)	0.5864(5)	0.1592(4)	0.5181(4)	0.0246
O(1)	0.5423(4)	0.0172(3)	0.1578(3)	0.0260	C(4)	0.4264(5)	0.2310(4)	0.3755(4)	0.0221
O(2)	0.6679(4)	0.0008(3)	0.2276(3)	0.0258	C(5)	0.3671(6)	0.2335(4)	0.2473(4)	0.0247
O(3)	0.6665(4)	0.1833(3)	0.2187(3)	0.0282	C(21)	0.7049(5)	0.4129(4)	1.0108(4)	0.0280
O(4)	0.7214(3)	0.0794(3)	0.4181(3)	0.0295	C(22)	0.5947(6)	0.3518(4)	1.0136(4)	0.0295
O(5)	0.7859(4)	0.0906(3)	0.6074(3)	0.0331	C(24)	0.4384(6)	0.2746(4)	0.8738(4)	0.0265
O(6)	0.3857(4)	0.2786(3)	0.4455(3)	0.0314	C(25)	0.3786(6)	0.2650(4)	0.7481(4)	0.0285
O(7)	0.8085(4)	0.6209(3)	0.1414(4)	0.0464	C(71)	0.1212(7)	0.4737(5)	1.0534(5)	0.0474
O(8)[b]	0.0246(24)	0.3099(17)	0.1726(17)	0.034(7)	C(72)	0.2995(5)	0.5774(4)	1.0311(4)	0.0361
O(21)	0.5452(4)	0.4812(3)	0.6431(3)	0.0271	C(73)	0.1060(6)	0.6333(5)	1.0988(5)	0.0408
O(22)	0.6690(4)	0.5028(3)	0.7104(3)	0.0273	C(74)	0.0975(5)	0.5855(4)	0.8936(4)	0.0350
O(23)	0.6750(4)	0.3213(3)	0.7175(3)	0.0298	C(75)	0.1679(9)	0.3970(5)	0.9838(7)	0.0769
O(24)	0.7189(4)	0.4386(3)	0.9086(3)	0.0284	C(76)	0.3786(6)	0.5639(5)	1.1508(4)	0.0462
O(25)	0.7767(4)	0.4375(3)	1.1000(3)	0.0404	C(77)	0.1235(7)	0.7297(5)	1.0752(6)	0.0618
O(26)	0.3985(4)	0.2257(3)	0.9485(3)	0.0307	C(78)	−0.0475(6)	0.5813(5)	0.8645(5)	0.0484
O(27)	0.7853(4)	0.9054(3)	0.6710(3)	0.0418	C(81)	0.1363(6)	1.0261(4)	0.5681(5)	0.0335
O(28)	0.0196(4)	0.2015(3)	0.6788(3)	0.0450	C(82)	0.2894(5)	0.9008(4)	0.5483(4)	0.0336
N(3)	0.5228(4)	0.1723(3)	0.3984(3)	0.0220	C(83)	0.0895(6)	0.8755(4)	0.6269(4)	0.0368
N(6)	0.4122(4)	0.1562(3)	0.1889(3)	0.0217	C(84)	0.0836(5)	0.9055(4)	0.4162(4)	0.0329
N(7)	0.1563(4)	0.5675(3)	1.0197(3)	0.0283	C(85)	0.1961(6)	1.0913(4)	0.4981(5)	0.0456
N(23)	0.5306(4)	0.3341(3)	0.8942(3)	0.0202	C(86)	0.3765(6)	0.9243(5)	0.6613(4)	0.0469
N(26)	0.4181(4)	0.3438(3)	0.6855(3)	0.0223	C(87)	0.0796(7)	0.7718(4)	0.6076(5)	0.0508
N(8)	0.1491(4)	0.9257(3)	0.5394(3)	0.0279	C(88)	−0.0596(6)	0.9209(5)	0.3881(5)	0.0458

[a] U_{eq} is the cube root of the product of the principal axes of the thermal ellipsoid. [b] Occupancy = 0.16(1).

Table 3. Selected Intramolecular Distances (Å) and Angles (deg) for $[NEt_4][VO(O_2)(GlyGly)]\cdot 1.58H_2O$ at 198 K

anion 1			anion 2		
		cor[a]			cor[a]
V(1)−O(1)	1.890(4)	1.892	V(2)−O(21)	1.895(4)	1.899
V(1)−O(2)	1.874(4)	1.877	V(2)−O(22)	1.900(4)	1.903
V(1)−O(3)	1.599(4)	1.601	V(2)−O(23)	1.580(4)	1.585
V(1)−O(4)	2.007(3)	2.009	V(2)−O(24)	2.006(3)	2.011
V(1)−N(3)	2.032(5)	2.035	V(2)−N(23)	2.029(4)	2.033
V(1)−N(6)	2.113(4)	2.117	V(2)−N(26)	2.106(4)	2.111
O(1)−O(2)	1.443(5)	1.446	O(21)−O(22)	1.431(5)	1.434
O(4)−C(1)	1.277(6)	1.279	O(24)−C(21)	1.301(6)	1.304
O(5)−C(1)	1.238(6)	1.239	O(25)−C(21)	1.227(6)	1.229
O(6)−C(4)	1.228(7)	1.230	O(26)−C(24)	1.276(7)	1.278
N(3)−C(2)	1.454(6)	1.456	N(23)−C(22)	1.464(6)	1.467
N(3)−C(4)	1.330(7)	1.332	N(23)−C(24)	1.303(8)	1.305
N(6)−C(5)	1.464(7)	1.466	N(26)−C(25)	1.484(7)	1.487
C(1)−C(2)	1.502(8)	1.505	C(21)−C(22)	1.484(8)	1.487
C(4)−C(5)	1.521(6)	1.522	C(24)−C(25)	1.502(7)	1.505
O(1)−V(1)−O(2)	45.09(16)		O(21)−V(2)−O(22)	44.32(15)	
O(1)−V(1)−O(3)	107.37(18)		O(21)−V(2)−O(23)	106.56(18)	
O(1)−V(1)−O(4)	121.88(18)		O(21)−V(2)−O(24)	119.40(17)	
O(1)−V(1)−N(3)	140.26(19)		O(21)−V(2)−N(23)	141.63(18)	
O(1)−V(1)−N(6)	78.73(17)		O(21)−V(2)−N(26)	78.80(16)	
O(2)−V(1)−O(3)	101.98(20)		O(22)−V(2)−O(23)	100.78(20)	
O(2)−V(1)−O(4)	79.99(16)		O(22)−V(2)−O(24)	78.96(15)	
O(2)−V(1)−N(3)	148.03(17)		O(22)−V(2)−N(23)	149.42(18)	
O(2)−V(1)−N(6)	123.78(16)		O(22)−V(2)−N(26)	123.11(16)	
O(3)−V(1)−O(4)	100.15(17)		O(23)−V(2)−O(24)	102.67(17)	
O(3)−V(1)−N(3)	102.88(21)		O(23)−V(2)−N(23)	102.50(21)	
O(3)−V(1)−N(6)	91.52(19)		O(23)−V(2)−N(26)	93.05(19)	
O(4)−V(1)−N(3)	76.11(16)		O(24)−V(2)−N(23)	76.81(16)	
O(4)−V(1)−N(6)	150.84(16)		O(24)−V(2)−N(26)	150.19(16)	
N(3)−V(1)−N(6)	75.26(16)		N(23)−V(2)−N(26)	75.12(16)	
V(1)−O(1)−O(2)	66.87(21)		V(2)−O(21)−O(22)	68.02(21)	
V(1)−O(2)−O(1)	68.04(22)		V(2)−O(22)−O(21)	67.66(22)	
V(1)−O(4)−C(1)	122.5(3)		V(2)−O(24)−C(21)	121.3(3)	
V(1)−N(3)−C(2)	118.4(3)		V(2)−N(23)−C(22)	118.2(4)	
V(1)−N(3)−C(4)	123.0(3)		V(2)−N(23)−C(24)	122.4(3)	
C(2)−N(3)−C(4)	118.4(4)		C(22)−N(23)−C(24)	119.3(4)	
V(1)−N(6)−C(5)	113.8(3)		V(2)−N(26)−C(25)	113.2(3)	
O(4)−C(1)−O(5)	123.1(5)		O(24)−C(21)−O(25)	123.0(5)	
O(4)−C(1)−C(2)	115.1(4)		O(24)−C(21)−C(22)	115.7(4)	
O(5)−C(1)−C(2)	121.8(5)		O(25)−C(21)−C(22)	121.4(5)	
N(3)−C(2)−C(1)	107.3(4)		N(23)−C(22)−C(21)	107.9(4)	
O(6)−C(4)−N(3)	126.7(4)		O(26)−C(24)−N(23)	126.6(4)	
O(6)−C(4)−C(5)	121.7(5)		O(26)−C(24)−C(25)	119.7(5)	
N(3)−C(4)−C(5)	111.7(5)		N(23)−C(24)−C(25)	113.7(5)	
N(6)−C(5)−C(4)	109.9(4)		N(26)−C(25)−C(24)	108.2(4)	

[a] Distances corrected for thermal motion using a rigid-body model for each ion.

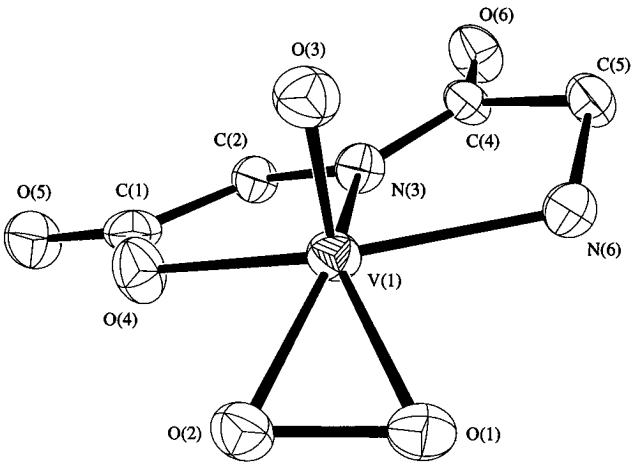

Figure 1. Molecular structure of $[VO(O_2)(GlyGly)]^-$. 50% probability thermal ellipsoids are shown for all non-hydrogen atoms of one of the two unique molecular anions in the crystal structure. Hydrogen atoms have been omitted.

Results and Discussion

The molecular structure of one of the independent complex anions of the dimer is shown in Figure 1. Bond distances and angles for the two independent anions are given in Table 3. The bonding geometry and dimensions are typical for oxovanadium(V) monoperoxo complexes[1,3,27,28] which frequently have the peroxide and three other coordinate atoms (in the present case both nitrogen atoms and a carboxyl oxygen atom of the deprotonated glycylglycinato ligand) approximately in a common plane with the V═O axial to this plane. The vanadium atom is somewhat displaced (∼0.4 Å) out of this approximate plane toward the doubly-bonded oxygen atom, and there is a weak interaction *trans* to the V═O bond.

The latter interaction is provided for in this case by the association of two independent anions—which are enantiomers—via weak V--O(peroxo) interactions about a pseudo-inversion center [V(1)--O(21)′ 2.660(4) Å; O(1)--V(2)′ 2.573(4) Å; O(3)-V(1)--O(21)′ 176.2(2)°; O(23)′-V(2)′--O(1) 176.6(2)°; where a prime denotes symmetry $(1 - x, -^1/_2 + y, 1 - z)$]. There is precedent for such linkages involving the peroxo ligand in the structure of $[O\{VO(O_2)_2\}_2]^{4-}$ [1] (V--O(peroxo) 2.522(3) and 2.480(2) Å)[2] and in $[PO_4\{VO(O_2)_2\}_2]^{5-}$ (V--O(peroxo) 2.351(4) and 2.411(4) Å).[18] Nonetheless, it is interesting that these relatively weak interactions occur in the present case in spite of other potential options for this axial "ligand" such as: water coordination as observed in $[NH_4][VO(O_2)(H_2O)(dipic)\cdot 1.3H_2O$ (2.211(2) Å) or coordination by a carbonyl oxygen of an adjacent anion as in $[NH_4][VO(O_2)(IDA)]$ (2.375(3) Å).[28] A weaker interaction has been observed when the interionic contact involves the vanadate oxygen (O═V) in the diperoxo anion in $[NH_4][VO(O_2)_2(NH_3)]$ (2.926(3) Å).[4]

There are four independent sites containing water of crystallization, one of which (O(8)) is only partly occupied (refined occupancy = 0.16(1)). Two of the independent water molecules (O(7) and O(27)) form hydrogen-bonds (O--O distances 2.729(6) Å to 2.843(6) Å) linking carbonyl oxygen atoms of the carboxyl and amide functions of adjacent anions. The other two water sites (O(28) and O(8)) are hydrogen-bonded to the first two water molecules respectively [O(7)--(H−)O(28)″ 2.781(6) Å; O(27)--(H−)O(8)″ 2.831(25) Å; where two primes denote symmetry $(1 - x, -^1/_2 + y, 1 - z)$]. O(28) is further hydrogen-bonded to the carbonyl oxygen atom of a carboxylate group [O(28)(-H)--O(5)‴ 2.956(6) Å; where three primes denote symmetry $(-1 + x, y, z)$]. The corresponding distance for O(8) [O(8)(−H)--O(25)^{iv} 3.216(26) Å; where iv denotes symmetry $(-1 + x, y, -1 + z)$] exceeds twice the van der Waals radius of oxygen[29] but may represent a weak hydrogen-bond. The net result of all these intermolecular interactions is a three-dimensionally extended structure regardless of whether or not O(8) is included. There are no other chemically significant intermolecular interactions. Figure 2 portrays stereoscopically an associated pair of anions and all of the water molecules which link this pair via hydrogen-bonds to other symmetry-related anions.

The $\{VO\}_2$ cyclic structure deriving from interactions between a vanadium atom of one center and an oxygen of a ligand in an adjacent center to form a dimeric structure represents a ubiquitous characteristic of vanadate chemistry. In complexes with 1,2-diols[30] and with α-hydroxy acids[31] such interactions are sufficiently strong that the dimeric structure is retained in aqueous solution while, with aliphatic alcohols in non-aqueous solution, an equilibrating mixture is established.[32]

On dissolution in water, the ^{51}V NMR spectrum showed a single signal at −649 ppm. This chemical shift is similar to those observed for peptide-based complexes that prevent the vanadium-catalyzed decomposition of hydrogen peroxide[17,21] and is the same as that of the corresponding glycylglycine complex.[22] Previous equilibrium studies have shown that the solution product is a monoperoxovanadate complex with a tridentate glycylglycine ligand,[21] after the fashion observed in the crystalline product described here. There seems little doubt that the aqueous monomeric unit of the crystalline dimer-like product and the solution product are structurally similar.

A question that arises concerning the solution product is whether the V--O (peroxo) bond joining the monomeric units of the dimer is replaced by a bond to a water oxygen in the solution product. Oxygen-17 NMR studies of diperoxovanadates have revealed coordinated water in aqueous solution.[15,33] Raman spectroscopic studies of diperoxo complexes have suggested that these compounds tend to have a pentagonal pyramidal coordination[34] as opposed to the pentagonal bipyramidal coordination that would arise if a water were coordinated in an apical position. On the other hand, pentagonal bipyramidal coordination is found in many monoperoxovanadate complexes.[1] Additionally, crystalline monoperoxovanadate complexes frequently have a water molecule coordinated in the apical position as, for instance, in the pyridine-2-carboxylate[35] complex of monoperoxovanadate and in a (pyridine-2,6-dicarboxylato)-monoperoxovanadate[3] complex. It, therefore, seems quite likely that, under aqueous conditions, water does occupy the seventh coordination site to give a solution structure very close to that of the complex in the crystalline state.

The ligand itself is unique in that a covalently bonded crystalline peptido complex of vanadate has not previously been reported. From the results of solution studies, it has previously been proposed that dipeptide complexes of vanadate[36−38] and

(27) Szentivanyi, H.; Stomberg, R. *Acta Chem. Scand.* **1983**, *A37*, 709−714.
(28) Djordjevic, C.; Craig, S. A.; Sinn, E. *Inorg. Chem.* **1985**, *24*, 1281−1283.
(29) Bondi, A. *J. Phys. Chem.* **1964**, *68*, 441−451.
(30) Angus-Dunne, S. J.; Batchelor, R. J.; Tracey, A. S.; Einstein, F. W. B. *J. Am. Chem. Soc.* **1995**, *117*, 5292−5296.
(31) Hambley, T. W.; Judd, R. J.; Lay, P. A. *Inorg. Chem.* **1992**, *31*, 343−345.
(32) Priebsch, W.; Rehder, D. *Inorg. Chem.* **1990**, *29*, 3013−3019.
(33) Howarth, O. W. *Prog. Nucl. Magn. Reson. Spectrosc.* **1990**, *22*, 453−485.
(34) Schwendt, P.; Pisarcik, M. *Spectrochim. Acta* **1990**, *46A*, 397−399.
(35) Mimoun, H.; Saussine, L.; Daire, E.; Postel, M.; Fischer, J.; Weiss, R. *J. Am. Chem. Soc.* **1983**, *105*, 3101−3110.

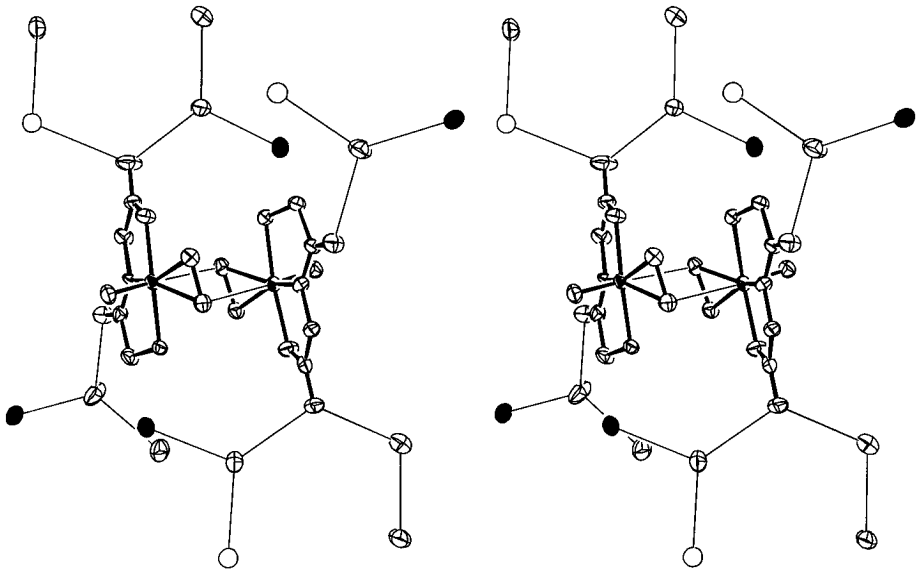

Figure 2. Stereodiagram showing an associated pair of anions and all directly associated water molecules and their hydrogen bonds. Hydrogen atoms are excluded. 50% probability thermal ellipsoids or spheres are shown. Thin lines are used to depict the interionic (V−O) interactions and the hydrogen-bonds (O−O). The 0.16(1)-occupied water sites (O(8)) are depicted by the open circles. The blackened ellipsoids represent carbonyl oxygen atoms from neighboring anions.

of monoperoxovandate[21,22] have tridentate coordination. This proposal has been confirmed by the present study. Additionally, the solution studies concluded that the amide nitrogen was deprotonated. This also is supported by this crystal structure in which the amide nitrogen atoms have a planar bonding environment. The sums of the bond angles about the amide nitrogen atoms, N(3) and N(23) are 359.8(6)° and 359.9(7)°, respectively (see Table 3).

A deprotonated amide in an oxovanadium(V) complex with 1,2-bis(2-hydroxy-2-methylpropanamide)benzene (OVHIBA) has been described.[39,40] The $V-N_{amide}$ bond lengths in this complex are 1.992(2) and 2.001(2) Å. In the glycylglycine complex the $V-N_{amide}$ bonds are slightly longer, V(1)−N(3) 2.032(5) Å and V(2)-N(23) = 2.029(4) Å (Table 3). This represents a small increase in bond length that may be a result of a number of factors, such as the expanded coordination sphere in the monoperoxide complex, specific electronic influences of the other ligands (pseudo trans influence) and constraints imposed by the differences in the fused ring systems of these complexes. Nevertheless, these $V-N_{amide}$ distances are markedly shorter than that in a closely related amino diacetate complex $[VO(O_2)(C_4H_5O_4N)]^-$ (V−N = 2.138(4) Å) in which the nitrogen atom is not deprotonated.[28]

Without additional data, it is difficult to know whether deprotonation of the amide nitrogen is characteristic of vanadium complexes of dipeptides and other amide-derived ligands with similar functionalities. The two available crystal structures show this for vanadate[39] and peroxovanadate (present work). In addition, solution studies of a number of dipeptides are consistent with this, both for vanadate[36−38] and for peroxovanadate.[21,22] The chemistry discussed here, for the monoperoxovanadate is quite different from that of diperoxovanadate where NMR studies of aqueous solutions have shown that reactions with peptides, amino acids and related compounds occur in a monodentate fashion to provide amino- and (carboxylato)-oxodiperoxovanadate derivatives.[20−22] Although, it seems likely that similar compounds are formed with monoperoxovandate, they have not yet been reported, even for conditions where they might have been expected.[20−22] This suggests that, if they are formed, they are relatively unfavored products.

The two types of complexes found for the mono- and bis-(peroxovanadates) suggests that these materials will have very different influences on the function of enzymatic materials. These differences will undoubtedly prove to be important for the study of the effects of peroxovanadates on phosphatases, kinases, and other phosphate-metabolizing enzymes. It can also be expected that the insulin-mimetic properties of peroxovanadates will be strongly biased by the number of peroxo ligands in the functional species.

Acknowledgment. Thanks are gratefully extended by F.W.B.E. and A.S.T. to the Natural Sciences and Engineering Research Council of Canada for its financial support of this work. We also wish to thank a reviewer for helpful comments concerning the discussion.

Supporting Information Available: Additional crystallographic details, hydrogen atom parameters, anisotropic thermal parameters, additional bond lengths and angles, torsion angles, and secondary interactions (10 pages). Ordering information is given on any current masthead page.

IC951007Y

(36) Tracey, A. S.; Jaswal, J. S.; Nxumalo, F.; Angus-Dunne, S. J. *Can. J. Chem.* **1995**, *73*, 489−498.
(37) Jaswal, J. S.; Tracey, A. S. *Can. J. Chem.* **1991**, *69*, 1600−1607.
(38) Rehder, D. *Inorg. Chem.* **1988**, *27*, 4312−4316.
(39) Cornman, C. R.; Zovinka, E. P.; Boyajian, Y. D.; Geiser-Bush, K. M.; Boyle, P. D.; Singh, P. *Inorg. Chem.* **1995**, *34*, 4213−4219.
(40) Cornman, C. R.; Geiser-Bush, K. M.; Singh, P. *Inorg. Chem.* **1994**, *33*, 4621−4622.